

# Target-Capture and Ion/Molecule Reactions in High-Energy Collisions between Protonated Polypeptide Ions and Hydrogen-Containing Target Gases

Xueheng Cheng and Catherine Fenselau\*

Contribution from the Department of Chemistry and Biochemistry, University of Maryland Baltimore County, Baltimore, Maryland 21228

Received December 9, 1992. Revised Manuscript Received April 20, 1993\*

**Abstract:** Product ions with masses above that of the precursor ion have been observed in high-energy collisions between protonated peptides  $MH^+$  with molecular weight ranging from 555 to 2585 and hydrogen-containing target gases ( $XH_n$ ) such as ammonia and methane. A major product ion observed had a mass corresponding to elimination of two hydrogens from the ion/target complex  $[MH + XH_n - 2H]^+$ . Incorporation of 14 Da,  $[CH_4 - 2H]$ , into fragment ions was observed in collision-induced dissociation (CID) of renin substrate with methane as the target gas. Optimum collision energies were shown to depend directly on the mass of the peptide ions and span from 12 to 24 eV in the center-of-mass frame. Isotope-labeling experiments established the origin of the two hydrogens eliminated from the ion/target complex, with one from the target and the other from the precursor ion. A mechanism based on homolytic bond breaking and re-formation in the ion/target complex formed by capturing the small target inside the relatively large ion was proposed to account for these experimental observations.

## Introduction

Collisions between accelerated gas-phase ions and target gases are processes significant to the study of collision-induced dissociation (CID) and ion/molecule reactions. CID is an important technique in tandem mass spectrometry (MS/MS).<sup>1</sup> It has been used extensively in the study of atomic/molecular interactions and energy-transfer processes and has been a routine method for structural determination in mass spectrometry.<sup>1</sup> The CID processes are usually divided, according to the collision energy employed, into those of high energy ( $E_{lab} \geq 1$  keV), which are accessible to sector instruments, and those of low energy ( $E_{lab} \leq 200$  eV), which are used mainly in quadrupole-based instruments and ion-trapping devices. The dynamics and mechanism of the CID process have been the subjects of numerous studies, and the behaviors of small systems are reasonably well understood.<sup>2</sup> The processes with large ions, on the other hand, are more difficult to study and, therefore, less understood. Rapid progress in the methods of ionizing large biomolecule ions has raised expectations for the application of CID in the structural analysis of large biomolecules.<sup>3</sup> One limitation of CID, however, is the low efficiency for dissociating large ions.<sup>2c,4</sup> A better understanding of the dynamics and mechanism of CID involving large ions is very important for improving dissociation efficiency and extending applications of CID.

Ion/molecule reactions usually take place in a low thermal energy collision between chemically reactive ions and target gases; these reactions involve ion/neutral complexes bound together mainly through electrostatic forces and are generally described

as orbiting complexes.<sup>5</sup> When collision energy is increased, the lifetime of the orbiting complexes decreases and so does the importance of the ion/molecule reaction.<sup>6</sup> Another type of ion/molecule reaction, the atom-stripping process, can take place in a high-energy collision without forming a long-lived ion/neutral complex, although this reaction is usually of low efficiency.<sup>7</sup>

In a study of high-energy CID of protonated peptides with He, Derrick and co-workers<sup>8</sup> measured the kinetic energy loss of the fragment ions. Using the assumption that the scattering angle of the target gas is close to  $0^\circ$ , they were able to calculate the velocity of the target relative to the projectile ion after collision and concluded that at an 8-keV collision with He, for peptides with molecular weight (MW) below and above 1500, the target was scattered forward and backward, respectively, in the center-of-mass frame. For peptides with MW close to 1500, their results predict no scattering of the target and a situation where, in effect, the target will be captured and an ion/neutral complex of a special kind will form. Recently, target-capture in high-energy CID has been observed for a special system, fullerene ions colliding with small target gases, independently by Schwarz and co-workers,<sup>9</sup> Gross and co-workers,<sup>10</sup> and Ross and co-workers.<sup>11</sup>

In this paper, we present evidence showing that target-capture in high-energy CID is likely to be a more general phenomenon.

(5) (a) Ausloos, P., Ed. *Interactions Between Ions and Molecules*; Plenum: New York, 1975. (b) Bowers, M. D.; Ed. *Gas Phase Ion Chemistry*; Academic: New York, 1979 and 1984.

(6) (a) Henchman, M. In *Ion-Molecule Reactions*; Franklin, J. L., Ed.; Plenum: New York, 1972; Vol. 1, pp 101-259. (b) Futrell, J. H.; Tiernan, T. O. In *Ion-Molecule Reactions*; Franklin, J. L., Ed.; Plenum: New York, 1972; Vol. 2, pp 485-552. (c) Orlando, R.; Fenselau, C.; Cotter, R. J. *J. Am. Soc. Mass Spectrom.* 1991, 2, 189-197.

(7) Davis, S. C.; Derrick, P. J.; Ottinger, C. Z. *Naturforsch., A; Phys. Sci.* 1990, 45, 1151-1157.

(8) Neumann, G. M.; Sheil, M. M.; Derrick, P. J. *Z. Naturforsch.* 1984, 39a, 584-592.

(9) Weiske, T.; Bohme, D. K.; Hrusak, J.; Kratschmer, W.; Schwartz, H. *Angew. Chem., Int. Ed. Engl.* 1991, 30, 884-886. (b) Weiske, T.; Hrusak, J.; Bohme, D. K.; Schwarz, H. *Chem. Phys. Lett.* 1991, 186, 459-462. (c) Weiske, T.; Schwarz, H. *Angew. Chem., Int. Ed. Engl.* 1992, 31, 605-606.

(10) (a) Caldwell, K. A.; Giblin, D. E.; Hsu, C. S.; Cox, D.; Gross, M. L. *J. Am. Chem. Soc.* 1991, 113, 8519-8521. (b) Caldwell, K. A.; Giblin, D. E.; Gross, M. L. *J. Am. Chem. Soc.* 1992, 114, 3743-3756.

(11) (a) Ross, M. M.; Callahan, J. H. *J. Phys. Chem.* 1991, 95, 5720-5723. (b) Mowrey, R. C.; Ross, M. M.; Callahan, J. H. *J. Phys. Chem.* 1992, 96, 4755-4761. (c) McElvany, S. W.; Ross, M. M.; Callahan, J. H. *Acc. Chem. Res.* 1992, 25, 162-168.

\* Abstract published in *Advance ACS Abstracts*, October 1, 1993.

(1) (a) McLafferty, F. W., Ed. *Tandem Mass Spectrometry*; Wiley: New York, 1983. (b) Busch, K. L.; Glish, G. L.; McLuckey, S. A. *Mass Spectrometry/Mass Spectrometry*; VCH: New York, 1988.

(2) (a) Shukla, A. K.; Qian, K.; Anderson, S.; Futrell, J. H. *J. Am. Soc. Mass Spectrom.* 1990, 1, 6-15. (b) McLuckey, S. A. *J. Am. Soc. Mass Spectrom.* 1992, 3, 599-614. (c) Gross, M. L. In *Methods in Enzymology*; McClosky, J. A., Ed.; Academic Press: San Diego, 1990; Vol. 193, pp 237-263.

(3) (a) Barinaga, C. J.; Edmonds, C. G.; Udseth, H. R.; Smith, R. D. *Rapid Commun. Mass Spectrom.* 1989, 3, 160-164. (b) Loo, J. A.; Edmonds, C. G.; Smith, R. D. *Anal. Chem.* 1991, 63, 2488-2499. (c) Orlando, R.; Boyd, R. K. *Org. Mass Spectrom.* 1992, 27, 151-155.

(4) Biemann, K. In *Methods in Enzymology*; McClosky, J. A., Ed.; Academic Press: San Diego, 1990, Vol. 193, pp 455-479.

In high-energy collisions of protonated peptides  $MH^+$  with hydrogen-containing targets ( $XH_n$ ), we observed product ions whose masses correspond to elimination of two hydrogens from the ion/target complex  $[MH + XH_n - 2H]^+$  and, in some cases, the ion/target complex itself,  $[MH + XH_n]^+$ . The incorporation of 14 Da,  $[CH_4 - 2H]$ , into the fragments from target methane was also observed in CID of renin substrate. The collision energy dependence study showed similarities to the fullerene system. This work renders experimental support to the analysis of collision dynamics of large peptide ions by Derrick and co-workers<sup>8</sup> and suggests a possible way for optimizing the efficiencies of energy conversion in CID and of dissociation of large ions. Moreover, the observation of product ions from target-capture at high energy implies that the conformation of gas-phase protonated polypeptides likely approaches spherical and that the ions are self-solvated.

## Experimental Section

**Instrumentation.** A JEOL (Tokyo, Japan) HX110/HX110 four-sector tandem mass spectrometer ( $E_1B_1E_2B_2$  geometry) was used in this work. The interface connecting MS1 ( $E_1B_1$ ) and MS2 ( $E_2B_2$ ) in the third field-free region (FFR) has been modified to improve ion transmission at low to intermediate kinetic energies (0–1000 eV).<sup>12</sup>

Precursor ions were generated using fast-atom bombardment (FAB) ionization (glycerol or thioglycerol matrix, 6-keV Xe atoms). The ions were accelerated to 10-keV ( $V_{acc}$ ) kinetic energy, mass-selected using MS1, decelerated by three cylindrical lenses, and injected into the collision cell located in the third FFR, where they collided with added target gases. The potential of the collision cell was set to  $V_{coll}$  to achieve the desired ion kinetic energy  $E_{lab} = e(V_{acc} - V_{coll})$ . The product and surviving precursor ions were reaccelerated to 10 keV and mass-analyzed using MS2.

Fullscan CID product spectra were obtained by linked scan at constant  $B_2/E_2$ . For these experiments MS1 was set to unit resolution and MS2 was set to 500 resolution.

In most of the experiments the masses of interest fell within 50 Da of the precursor ion. This narrow mass range could be scanned magnetically ( $B$ ) at a constant  $E$  value in MS2 when the  $B$ -slit was opened.<sup>13</sup> Magnetic scanning was preferred because it is easier to obtain high resolution when  $B$  scanning is used instead of linked  $B/E$  scanning. In this case both MS1 and MS2 were set to provide better than unit resolution at 10% valley.

In CID experiments using deionized  $H_2O$  or  $CH_3OH$  as collision targets, the target was introduced into the collision cell using a direct insertion probe equipped with a solvent reservoir.

**Materials.** Peptides [Leu]enkephalin, [Leu]enkephalin-arginine, and valinomycin were obtained from Sigma Chemical Co. (St. Louis, MO), and renin substrate, ACTH(22–39), and melittin were obtained from Bachem (Torrance, CA). The peptides were dissolved in 0.1% trifluoroacetic acid (TFA) (1–2 mg/mL) before use. Collision gases He, Ar,  $NH_3$ ,  $CH_4$ ,  $CO_2$ ,  $CH_3NH_2$ , and  $Me_2NH$  were obtained from Matheson Gas Products (Secaucus, NJ). Isotope-labeled gas  $ND_3$  was from MSD Isotopes (Montreal, Canada) (99.4 atom % D), and  $CD_4$  was from Isotech Inc. (Miamisburg, OH) (99 atom % D). A gas mixture of  $CH_4/CD_4$  was prepared by mixing the two gases in a length of tubing separated from the gas tanks and the collision cell by two- and three-way valves.

**Hydrogen–Deuterium Exchange.** H/D exchange of renin substrate in solution was carried out by dissolving the peptide (5.0 mg) in an excess of deuterium oxide (5.0 cm<sup>3</sup>) (Sigma Chemical Co., 99.5%) followed by lyophilization. This process was repeated three times. The FAB matrix, thioglycerol, was mixed with an equal volume of deuterium oxide on the FAB probe tip, followed by evacuation, and this process was repeated three times. The  $[M - 25H + 26D]^+$  ion was the most abundant in the resulting population of isotopomers, and it was further enriched as the precursor ion by selection with unit resolution in MS1.

## Results

### I. Reaction of Renin Substrate with Ammonia and Methane.

When mass-selected protonated renin substrate (DRVYIHPF-HLLVYS, MW = 1758) was injected into the collision cell at

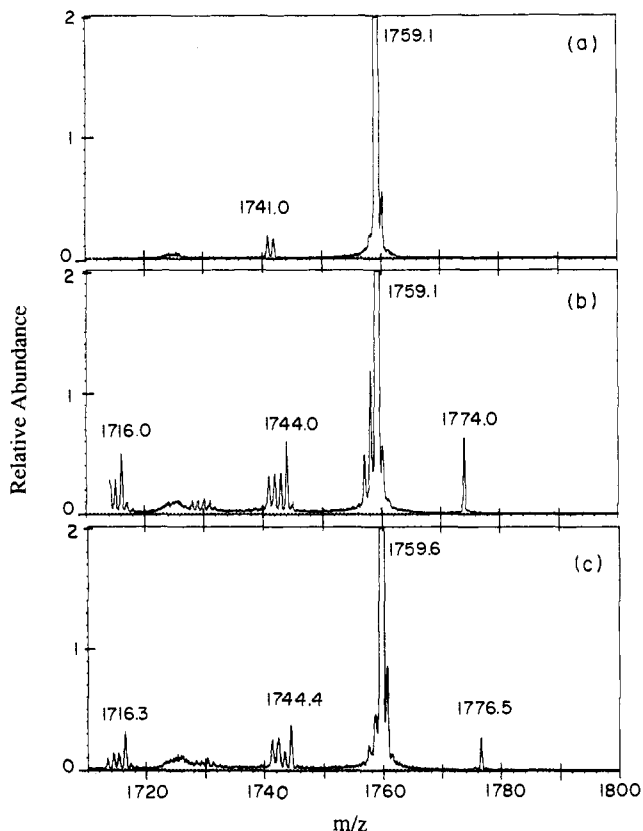


**Figure 1.** Product ion spectra in the precursor ion region from the collision of protonated renin substrate at  $E_{lab} = 2.2$  keV with (a) no collision gas added; (b)  $NH_3$  as collision gas; and (c)  $ND_3$  as collision gas.

a collision energy ( $E_{lab}$ ) of 2.2 keV with ammonia added as collision gas at a pressure that attenuates the precursor ions by 30%, a peak was observed with a mass 15 Da above that of the precursor, assigned as  $[MH + NH_3 - 2H]^+$  (Figure 1b). When no collision gas was added, no ion with a mass above that of the precursor was observed (Figure 1a). The other peaks seen in spectrum 1a occur at  $m/z$  1741 and 1742 and represent ions (presumably  $[MH - 17]^+$  and  $[MH - 18]^+$ ) formed by metastable decompositions in the collision cell. A broad peak centered at  $m/z$  1725 reflects metastable ion decomposition between  $E_2$  and  $B_2$  sectors. The addition of  $NH_3$  produces fragment ions corresponding to  $[MH - 1]^+$ ,  $[MH - 2]^+$ ,  $[MH - 14]^+$ ,  $[MH - 15]^+$ , and ions of lower masses which were not present in spectrum 1a. Most of those fragment ions are seen in CID spectra with He or Ar as collision targets and therefore are normal CID fragments. The yield of the  $[MH + NH_3 - 2H]^+$  ion depends on both the pressure of  $NH_3$  and the collision energy. Figure 2 shows the variation of the yield of  $[MH + NH_3 - 2H]^+$  vs the attenuation of the precursor ion, which is proportional to the pressure of  $NH_3$ . As the pressure of  $NH_3$  increases, the yield of the  $[MH + NH_3 - 2H]^+$  ion (relative to attenuated  $MH^+$ ) increases sharply until the attenuation of  $MH^+$  reaches 30%, after which this increase slows down possibly because multiple collisions cause dissociation of the  $[MH + NH_3 - 2H]^+$  ion. When the collision energy was varied, a maximum yield of the  $[MH + NH_3 - 2H]^+$  ion was observed at  $E_{lab} = 2.2$  keV ( $E_{cm} = 21.0$  eV) (Figure 3) with an abundance of 0.7% relative to  $MH^+$ . Also, when the collision energy was decreased to below  $E_{lab} = 2.0$  keV, a new, less abundant product ion appeared, which corresponds to the ion/target complex itself,  $[MH + NH_3]^+$  (Figure 3). The ion/target complex showed a maximum yield at  $E_{lab} = 1.3$  keV ( $E_{cm} = 12.4$  eV). The pressure dependence of the ion/target complex was similar to that of the major product,  $[MH + NH_3 - 2H]^+$ .

When protonated renin substrate was reacted with  $CH_4$ , a product ion with mass  $[MH + 14]^+$  was observed (Figure 4b)

(12) Cheng, X.; Wu, Z.; Fenselau, C.; Ishihara, M.; Musselman, B. D. *J. Am. Soc. Mass Spectrom.*, submitted for publication.

(13) Hill, J. A.; Biller, J. E.; Martin, S. A.; Biemann, K.; Yoshidome, K.; Sato, K. *Int. J. Mass Spectrom. Ion Process* 1989, 92, 211–230.

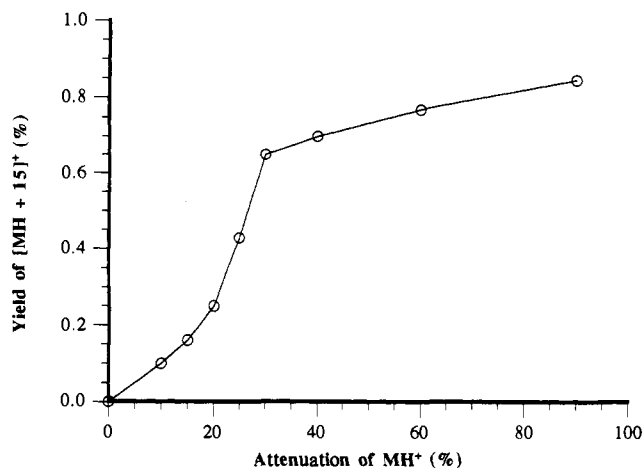


**Figure 2.** Plot of the yield of the  $[MH + 15]^+$  ion from the collision of protonated renin substrate with  $NH_3$  at  $E_{lab} = 2.2$  keV versus the attenuation of the precursor ion.

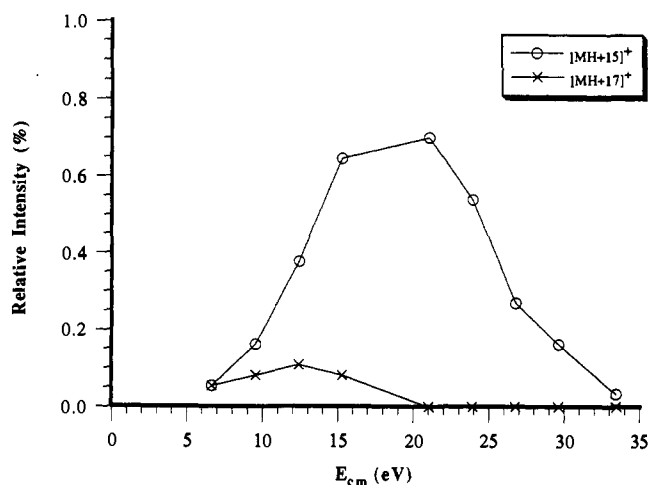


**Figure 3.** Plot of the yield of the  $[MH + 15]^+$  and  $[MH + 17]^+$  ions from the collision of protonated renin substrate with  $NH_3$  versus the collision energy in the center-of-mass frame.

and was assigned as  $[MH + CH_4 - 2H]^+$ . Another product ion with a mass 2 Da higher, corresponding to the ion/target complex  $[MH + CH_4]^+$ , was observed at lower collision energies (Figure 5) similar to the reaction of  $NH_3$ . Also similar to the reaction of  $NH_3$  was the dependence of the yield of  $[MH + CH_4 - 2H]^+$  on the pressure of  $CH_4$  and the collision energy. A maximum yield of 0.7% relative to  $MH^+$  was achieved at  $E_{lab} = 2.4$  keV ( $E_{cm} = 21.6$  eV), as shown in Figure 5.

In order to determine the source of the two hydrogens eliminated from the ion/target complex, isotope-labeling experiments were performed. When protonated renin substrate was reacted with a mixture of  $CH_4/CD_4$  at  $E_{lab} = 2.4$  keV, two peaks were observed with masses above that of the precursor ion corresponding to  $[MH + 14]^+$  and  $[MH + 17]^+$  and were assigned as  $[MH + CH_4 - 2H]^+$  and  $[MH + CD_4 - H - D]^+$ , respectively (Figure 4c). Separate experiments using pure  $CD_4$  gave  $[MH + CD_4 - H - D]^+$  as the only ion heavier than the precursor (data not shown). When  $ND_3$  was used at  $E_{lab} = 2.2$  keV,  $[MH + 18]^+$  was the only product ion with a mass above that of the precursor (Figure 1c), which was assigned as  $[MH + ND_3 - H - D]^+$ , similar to the reaction with  $CD_4$ . The absence of  $[MH + XD_n - 2H]^+$  and  $[MH + XD_n - 2D]^+$  indicates the specificity of the process of eliminating (H,D) from the ion/target complex.

Isotope-labeling experiments were also done in which the active hydrogens (there are 25 hydrogens attached to O and N atoms in this peptide; all are readily exchangeable in solution) in renin substrate were exchanged for deuterium in solution and the

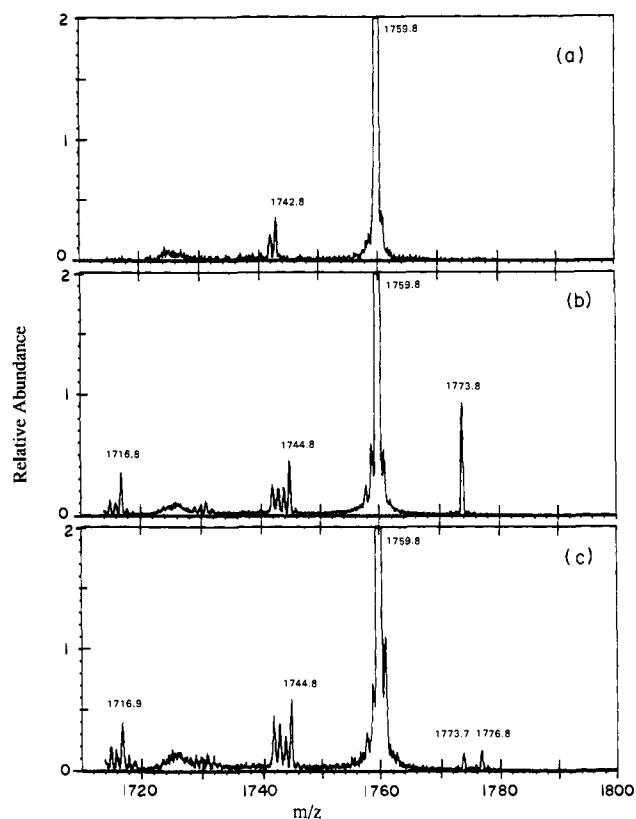


**Figure 4.** Product ion spectra in the precursor ion region from the collision of protonated renin substrate at  $E_{lab} = 2.4$  keV with (a) no collision gas added; (b)  $CH_4$  as collision gas; and (c) a mixture of  $CH_4$  and  $CD_4$  as collision gas.

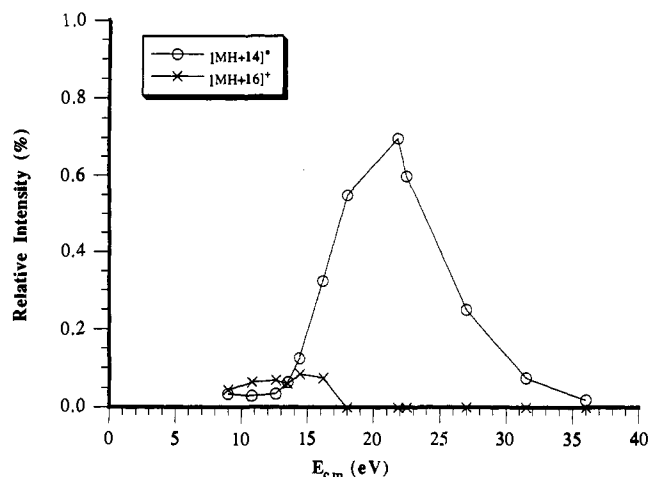


**Figure 5.** Plot of the yield of the  $[MH + 14]^+$  and  $[MH + 16]^+$  ions from the collision of protonated renin substrate with  $CH_4$  versus the collision energy in the center-of-mass frame.

perdeuterated precursor ion  $[M - nH + (n + 1)D]^+$ ,  $n = 25$ , was selected for the reaction. When  $CH_4$  and  $CD_4$  were used as collision gases, product ions corresponding to  $[M - nH + (n + 1)D + 14]^+$  and  $[M - nH + (n + 1)D + 17]^+$  were observed (Table I), respectively. These ions were assigned as  $[M - nH + (n + 1)D + CH_4 - 2H]^+$  and  $[M - nH + (n + 1)D + CD_4 - H - D]^+$ , respectively. These results suggest that the incorporation of target does not take place at sites involving exchangeable hydrogens.

Incorporation of target gas into the fragment ions was also examined. When full scan CID spectra of renin substrate were recorded at  $E_{lab} = 3.0$  keV with He,  $CH_4$ , or  $CD_4$  as target gases, incorporation of 14 Da ( $CH_4$  target gas) and 17 Da ( $CD_4$  target gas) into some of the fragment ions was observed. Figure 6 shows

**Table I.** Summary of Products from Reactions of Protonated and Deuterated Renin Substrate with NH<sub>3</sub>, CH<sub>4</sub>, and Their Deuterated Analogs in High-Energy Collisions

precursor	target	products	
		mass	assigned composition
no deuterium	NH <sub>3</sub>	MH + 15	MH + NH <sub>3</sub> - 2H
		MH + 17	MH + NH <sub>3</sub>
	ND <sub>3</sub>	MH + 17	MH + ND <sub>3</sub> - H - D
		MH + 14	MH + CH <sub>4</sub> - 2H
	CH <sub>4</sub>	MH + 16	MH + CH <sub>4</sub>
		m <sub>j</sub> + 14 <sup>a</sup>	m <sub>j</sub> + CH <sub>4</sub> - 2H
		MH + 17	MH + CD <sub>4</sub> - H - D
	CD <sub>4</sub>	m <sub>j</sub> + 17	m <sub>j</sub> + CD <sub>4</sub> - H - D
		CH <sub>4</sub> /CD <sub>4</sub>	MH + 14
	deuterated	CH <sub>4</sub>	MH + 17
M - 25H + 26D + 14			26D + CH <sub>4</sub> - 2H
CD <sub>4</sub>		M - 25H + 26D + 17	M - 25H + 26D + CD <sub>4</sub> - H - D

<sup>a</sup> m<sub>j</sub> is a series of a<sub>n</sub> fragment ions.

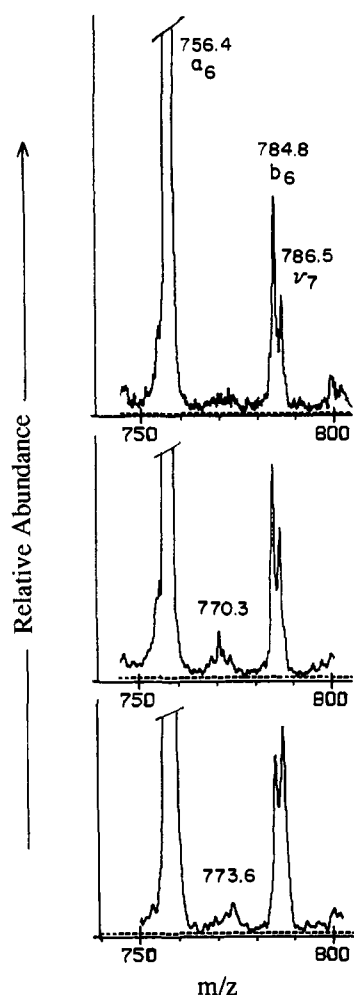


**Figure 6.** Product ion spectra in the region of  $m/z$  750–800 from the collision of protonated renin substrate at  $E_{lab} = 3.0$  keV with (a, top) He as collision gas; (b, middle) CH<sub>4</sub> as collision gas; and (c, bottom) CD<sub>4</sub> as collision gas.

the product ion spectra in the  $m/z$  750–800 region for He (a), CH<sub>4</sub> (b), and CD<sub>4</sub> (c) as collision gas. The incorporation of 14 Da (6b) and 17 Da (6c) into fragment ion a<sub>6</sub> (the nomenclature follows that of Roepstorff and Fohlman,<sup>14a</sup> modified by Biemann<sup>14b</sup>) can be seen, with the latter being somewhat less abundant than the former. These mass increments are identical

(14) (a) Roepstorff, P.; Fohlman, J. *Biomed. Mass Spectrom.* 1984, 11, 601. (b) Biemann, K. *Biol. Environ. Mass Spectrom.* 1988, 16, 99–111.

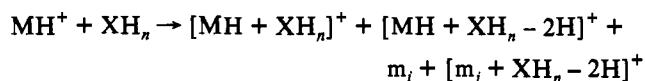
**Table II.** Optimal Collision Energies and Yields of [MH + XH<sub>n</sub> - 2H]<sup>+</sup> Ions from Reaction of Various Peptides with NH<sub>3</sub> and CH<sub>4</sub>

peptides	MW <sup>a</sup>	XH <sub>n</sub>	optimal collision energy			D(Å) <sup>c</sup>
			$E_{lab}$ (keV)	$E_{cm}$ (eV)	yield (%) <sup>b</sup>	
melittin	2846	NH <sub>3</sub>	4.0	23.8	2.4	21.2
		CH <sub>4</sub>	4.2	23.5	2.4	21.2
ACTH(22–39)	1986	CH <sub>4</sub>	2.6	20.8	1.0	19.8
		NH <sub>3</sub>	2.2	21.0	0.7	18.0
renin sub.	1759	CH <sub>4</sub>	2.4	21.6	0.7	18.0
		NH <sub>3</sub>	1.2	18.1	0.2	15.5
[Leu]Enk-Arg	172	NH <sub>3</sub>	0.63	14.5	0.1	13.3
[Leu]Enk	556	NH <sub>3</sub>	0.40	11.9	<0.05	12.3

<sup>a</sup> Molecular weight of MH<sup>+</sup>. <sup>b</sup> Relative to MH<sup>+</sup>. <sup>c</sup> Estimated thickness of the protonated peptides in the gas phase; see text for details.

to the incorporation of 14 and 17 Da into the precursor ion when CH<sub>4</sub> and CD<sub>4</sub> were used as target gases, respectively (Figure 4). Furthermore, for the precursor ion, CD<sub>4</sub> also gives less abundant incorporation product than CH<sub>4</sub>. Satellite ions appearing when CH<sub>4</sub> or CD<sub>4</sub> was added as target gas include a<sub>12</sub>, a<sub>9</sub>, a<sub>8</sub>, a<sub>6</sub>, a<sub>5</sub>, and a<sub>4</sub>.

The results for reaction of renin substrate discussed so far can be summarized by



where [MH]<sup>+</sup> is the protonated peptide, XH<sub>n</sub> is the collision target, m<sub>i</sub> represents fragment ions with masses lower than that of the precursor, and m<sub>j</sub> is a subset of m<sub>i</sub>. When He or Ar was used as the collision gas, no peak with a mass above that of the precursor was observed.

The above results of the reaction of protonated renin substrate with ammonia and methane are summarized in Table I.

Reactions of protonated renin substrate with H<sub>2</sub>O, CH<sub>3</sub>OH, CH<sub>3</sub>NH<sub>2</sub>, (CH<sub>3</sub>)<sub>2</sub>NH, and CO<sub>2</sub> were also investigated. Preliminary results indicate that, in each case, one or more product ions with masses above that of the precursor were observed. However, these ions' intensities were very weak, which did not permit more detailed study.

**II. Reaction of Other Peptides.** In addition to renin substrate, several other peptides including [Leu]enkephalin (YGGFL, MW = 555), [Leu]enkephalin-arginine (YGGFLR, MW = 711), valinomycin<sup>15</sup> (MW = 1111), ACTH(22–39) (VYPNGAEDE-SAEAFDLEF, MW = 1950), and melittin (GIGAVLKVLT-TGLPALISWIKRKRQQ-NH<sub>2</sub>, MW = 2585) were also studied. In each case, a product ion corresponding to [MH + XH<sub>n</sub> - 2H]<sup>+</sup> was observed (XH<sub>n</sub> = NH<sub>3</sub> and/or CH<sub>4</sub>). The collision energy dependence, however, was different for each peptide studied. Peptides with lower MW showed an optimal collision energy lower than that for peptides with higher MW. The maximum yield of [MH + XH<sub>n</sub> - 2H]<sup>+</sup> ions was also different for each peptide studied. There seemed to be a direct correlation between the MW of the peptides and the maximum yield of the [MH + XH<sub>n</sub> - 2H]<sup>+</sup> ion for the six peptides studied with NH<sub>3</sub> and CH<sub>4</sub> as the collision gases.

When [Leu]enkephalin-arginine was reacted with NH<sub>3</sub> at collision energies below optimal for the formation of the [MH + NH<sub>3</sub> - 2H]<sup>+</sup> ion, another weak product ion corresponding to [MH + NH<sub>3</sub>]<sup>+</sup> was observed. The optimal collision energy ( $E_{lab}$ ) for this ion was 400 eV ( $E_{cm} = 9.3$  eV), lower than that for the [MH + NH<sub>3</sub> - 2H]<sup>+</sup> ion ( $E_{lab} = 630$  eV,  $E_{cm} = 14.5$  eV). These observations were very similar to those for reactions of renin substrate with NH<sub>3</sub> and CH<sub>4</sub>.

(15) Valinomycin is a cyclic polymer with both amide and ester bonds.

Reactions of doubly protonated melittin with  $\text{CH}_4$  were also examined. The collision energy dependence and the yield of the incorporation product for doubly protonated melittin were very similar to those for singly protonated melittin. Because doubly protonated melittin had twice as much charge as singly protonated melittin, the difference between the acceleration voltage of MS1 ( $V_{\text{acc}} = 10$  kV) and the voltage of the collision cell ( $V_{\text{coll}}$ ) where maximum target incorporation was observed was 2.1 kV for the former and 4.2 kV for the latter.

## Discussion

The incorporation of target atoms into the product ions in high-energy CID has been observed only rarely. To date, the examples are those with transfer of a single atom (usually H) from the target to the precursor through the atom-stripping process.<sup>16</sup> The facts that chemically inert gases (He, Ar, Xe,  $\text{N}_2$ , for example) are usually employed as targets in CID, that most of the high-energy CID studies are performed at single-collision energy, and that the target-capture complex may have internal energy too high for the complex to survive before reaching the detector are likely reasons for the lack of observation of target-atom incorporation. The recent reports<sup>9-11</sup> that in high-energy CID of fullerenes incorporation occurs of small target atoms into fragments and into the fullerene precursor ions themselves are relevant. Fullerenes have cage-like structure and, therefore, are ideal traps for small targets. Once trapped, it is difficult for the target to escape. The stable cage structure of fullerenes also accommodates the internal energy generated from target-trapping well enough for the endohedral complex to be detected. The apparent dissimilarity between polypeptide and cage-like fullerenes and the large amounts of internal energy that the polypeptide ion/target complex must accommodate in order to be detected intact made the observations reported here unexpected. However, several lines of evidence support target-capture as the process responsible for the observations in this work. First, the energy dependence for formation of products with masses above the precursor in this work is very similar to that observed for the formation of an endohedral complex in CID of  $\text{C}_{60}^+$  with He.<sup>11b</sup> The optimal collision energy for the formation of ion/target complexes is somewhat lower than that for the formation of  $[\text{MH} + \text{XH}_n - 2\text{H}]^+$  ions, the incorporation product. This observation suggests that target-capture complexes are formed at low collision energies ( $E_{\text{cm}} \approx 10$  eV), and when the collision energy is increased, the excess energy causes dissociation of the complexes, giving rise to the  $[\text{MH} + \text{XH}_n - 2\text{H}]^+$  product. Second, the observation of the ion/target complex and, more importantly, of incorporation of 14 and 17 Da into the fragment ions in CID of renin substrate with  $\text{CH}_4$  and  $\text{CD}_4$  demonstrates target-capture. Third, elimination of (H, D) from the ion/target complex with a deuterated target suggests that the interaction time between the ion and the target during collision is longer than a simple atom-stripping process. Fourth, increase in the optimal collision energy ( $E_{\text{cm}}$ ) for the formation of the incorporation product with an increase in MW of the polypeptides indicates that the process is sensitive to the size (thickness) of the ion.

The threshold energies for the observation of  $[\text{MH} + \text{XH}_n - 2\text{H}]^+$  and  $[\text{MH} + \text{XH}_n]^+$  ions are around 7–10 eV ( $E_{\text{cm}}$ ) in this work. The existence and values of these threshold energies clearly ruled out the possibility of an ion/target complex formed by electrostatic interactions, or the orbiting complex. These threshold values are roughly twice the value for covalent bond strength for single bonds. Thus, the collision energy at which the target-capture product was observed is enough for the homolytic cleavage of covalent bonds.

The values of maximum yield and optimal collision energy for different peptides vary (Table II). The higher the MW of the

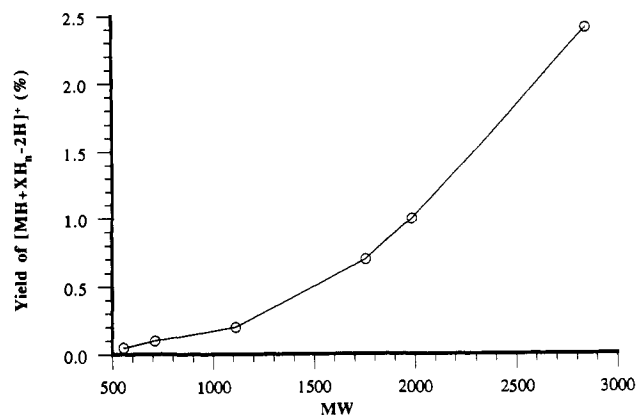


Figure 7. Plot of the maximum yield of the  $[\text{MH} + \text{XH}_n - 2\text{H}]^+$  ion ( $\text{XH}_n = \text{NH}_3$  and/or  $\text{CH}_4$ ) for the six peptides studied versus the molecular weight of the peptides (data from Table II).

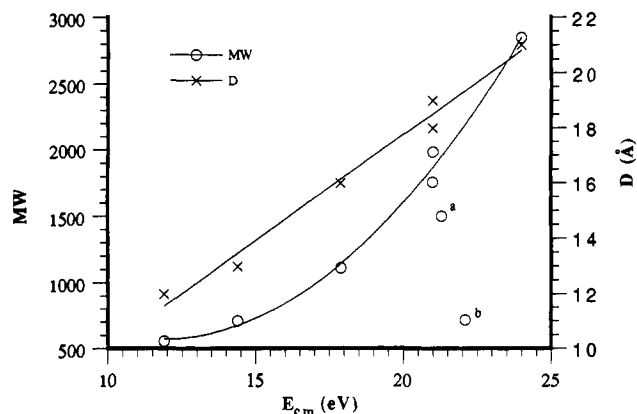


Figure 8. Plot of the molecular weight and the estimated thickness<sup>17</sup> of the six peptides studied versus the optimal collision energy ( $E_{\text{cm}}$ ) for the formation of the  $[\text{MH} + \text{XH}_n - 2\text{H}]^+$  ion ( $\text{XH}_n = \text{NH}_3$  and/or  $\text{CH}_4$ ) (data from Table II). Points a and b represent data adopted from ref 8 and 10b, respectively. See text for details.

peptide is, the larger the maximum yield and optimal collision energy (both  $E_{\text{lab}}$  and  $E_{\text{cm}}$ ) become. These trends can be seen more readily from Figures 7 and 8. In Figure 7, the maximum yield of the incorporation product is plotted against the MW of the peptides; in Figure 8, the MW and thickness of the peptides, estimated using a spherical model of constant density,<sup>17</sup> are plotted against the optimal collision energies ( $E_{\text{cm}}$ ). Since MW has been considered in using  $E_{\text{cm}}$  instead of  $E_{\text{lab}}$ , these correlations are likely valid with the cross section and the thickness of the peptide ions. If the cross section of the peptides is the only factor, it is predicted that, with an increase in MW, only the yield of product will increase but not the optimal collision energy in the center-of-mass frame. In fact, Figure 7 does suggest a linear correlation between the yield of  $[\text{MH} + \text{XH}_n - 2\text{H}]^+$  and the cross section of the peptides ( $\text{MW}^{2/3}$ ). Thus, the factor most likely affecting the optimal collision energy is suggested to be the thickness of the ion. In Figure 8, a linear correlation with the optimal collision

(17) The thickness of the isolated, protonated peptides in the gas phase is estimated assuming a constant density and spherical conformation for all the peptides. Thus,  $D = (6V/\pi)^{1/3} = [6(\text{MW})/\pi\rho]^{1/3} = [C(\text{MW})]^{1/3}$ , where  $D$  is the thickness of the peptide (diameter of the peptide with the assumption of spherical conformation),  $V$  is the volume of the peptide,  $\rho$  is the density of the peptide, and  $C = 6/\pi\rho$  is a constant whose value depends on that of  $\rho$ . A value of  $C = 10/\pi$  ( $\rho = 0.6 \text{ Da } \text{Å}^{-3}$ ) is adopted by fitting the thickness to the MW of several peptides (data from theoretical studies) and small proteins (crystallographic data) including enkephalins [(a) Isogai, Y.; Nemethy, G.; Scheraga, H. A. *Proc. Natl. Acad. Sci. U.S.A.* 1977, 74, 414–418]; bradykinin [(b) Galaktinov, G. S.; Sherman, S. A.; Shenderovich, M. D.; Nikiforovich, G. V.; Leonova, V. I. *Bioorg. Khim.* 1977, 3, 1190–1197]; LH-RH and analogues [(c) Momany, F. A. *J. Am. Chem. Soc.* 1976, 98, 2990–2996. (d) Momany, F. A. *J. Am. Chem. Soc.* 1976, 98, 2996–3000]; and lysozymes and myoglobins [(e) Cantor, C. R.; Schimmel, P. R. *Biophysical Chemistry*; Freeman: New York, 1980].

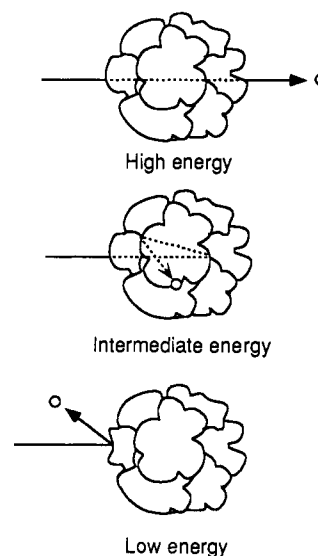
(16) (a) Dotan, I.; Lindinger, W. *J. Chem. Phys.* 1982, 76, 4972–4977. (b) Ervin, K. M.; Armentrout, P. B. *J. Chem. Phys.* 1985, 83, 166–189.

energy ( $E_{cm}$ ) was found for the thickness of the peptides but not for their MW. In the work of Derrick and co-workers,<sup>8</sup> at constant collision energy ( $E_{lab} = 8$  keV), the kinetic energy loss of the fragment ions was interpreted as showing that the target changes from forward scattering to backward scattering in the center-of-mass frame, when the MW of peptides is increased to ca. 1500. This change of scattering indicates that the dynamics of the collision changes from the target going through the ion to the target deflecting back from the ion. When the MW is increased, the value of  $E_{cm}$  will decrease and the thickness of the peptide will increase. Both of these changes will affect the dynamics of collision. If a hypothetical peptide with a MW of 1500 is plotted in Figure 8 in collision with He at  $E_{lab} = 8$  keV ( $E_{cm} = 21.3$  eV), the point is off the line fitting the data from this work by ca. 2 eV (higher in  $E_{cm}$ ). Considering that, due to the increased dissociation of the target-capture complex at increased collision energy, the points for this work, which represent the collision energy at which maximum yield of target incorporation was observed, will be lower than the true collision energy at which the optimal amount of target-capture will be formed, the agreement may in fact be better than that suggested in Figure 8. A similar argument was put forward in explaining the difference between the optimal collision energy for the observation of  $C_{60}He^+$  from experiments and for the formation of  $C_{60}He^+$  from molecular dynamics simulation.<sup>11b</sup> If the results for  $C_{60}He^+$  were plotted in Figure 8, they would be far off the line (about 8 eV<sup>10b</sup> higher in  $E_{cm}$ ). Because of the rigid structure of  $C_{60}$ , it may be more difficult for the target to get into and get out of the cage compared with peptides.

When the mass of the ion becomes extremely large, the situation will approach the limit of ion/surface collision. That is, beyond some point, the further increase of collision energy will not change the dynamics of the collision because the ion in this case is too thick. In that situation, target-capture in CID might be thought of as equivalent to the ion sticking to the surface in an ion/surface collision, and the elimination of 2H from the ion/target complex in this work would equal surface-induced dissociation or, more accurately, part of the projectile ion sticking to the surface.

The size dependence of target-capture in peptide ions raises the question of the shape and exact size of these gas-phase ions. Unfortunately, no experimental information concerning the conformation of large gas-phase ions has yet emerged. Increased cross section for precursor ion attenuation in CID of larger peptide ions indicates an increased physical cross section.<sup>18</sup> Increased basicity values measured for higher oligomers of glycine show that the proton is increasingly well self-solvated in this series of homologues,<sup>19a</sup> and a large negative entropy effect observed in dissociation of proton-bound dimers containing peptides GGG or GGGG indicates the existence of intramolecular H-bonding in those protonated peptides.<sup>19b</sup> H/D exchange of protonated peptides and multiply protonated proteins, generated from fast-atom bombardment<sup>20a</sup> and electrospray ionization,<sup>20b</sup> is interpreted to suggest the accessibility of only part of the exchangeable hydrogen atoms in the peptide and protein ions to the exchanging reagent. Apparent dependence of charge states in the multiply charged ions generated by electrospray in folded versus denatured protein samples suggests the different conformations that these

## Scheme I



protein ions might have in the gas phase.<sup>21</sup> These observations all point to the complicated conformations that gas-phase ions of moderate to large size can assume. For the sake of the present discussion, we propose that the protonated peptides studied in this work assume gas-phase conformations as roughly spherical aggregations, in which the primary peptide backbone wraps around to solvate the proton inside the ball. This "loose-woolen-ball" model for gas-phase protonated peptides will be shown to give a satisfactory explanation for the experimental observations and to offer a convenient model for the description of a more detailed mechanism of the target-capture and reaction in high-energy collision of protonated peptides with hydrogen-containing targets in this work.

A schematic representation of the target-capture process in CID of protonated peptides is given in Scheme I, in which collisions with a relatively small impact parameter (head on) are chosen. The validity of this choice has been justified elsewhere.<sup>8</sup> For the convenience of drawing, the peptide in Scheme I is shown to be static and the target moving. At low collision energies (a), which will not permit the penetration of the target into the projectile ion or cleavage of any bond, the target will be deflected structurally intact. At very high collision energies (c), the target will penetrate through the ion with or without breaking bonds. At appropriate intermediate collision energies (b), the target will be able to just penetrate into the ion without being able to go through it. This is the situation where an ion/target complex can be formed at a high-energy collision. Scheme II presents proposed mechanisms for the formation of the product ions observed in this work. As mentioned before, the collision energies at which these product ions are observed are more than enough to break covalent bonds homolytically. After the relative velocity of the target is brought close to 0 by deflection and/or breaking bonds, the target and the ion will coexist for a certain length of time during which reaction can take place. In principle, the observed products could be formed by concerted or stepwise processes. At this stage, we do not have enough experimental evidence to disprove either one. However, the specific elimination of (H, D), when a deuterated target was used, indicates that the reaction intermediate does not live long enough for normal isotope exchange, as observed in ion/molecule reactions that take place at low thermal energy.<sup>20,22</sup> A direct mechanism similar to the concerted process proposed here has been suggested for the surface adsorbant pickup reaction

(18) Neumann, G. M.; Derrick, P. J. *Org. Mass Spectrom.* **1984**, *19*, 165–170.

(19) (a) Wu, Z.; Fenselau, C. *J. Am. Soc. Mass Spectrom.* **1992**, *3*, 863–866. (b) Cheng, X.; Wu, Z.; Fenselau, C. *J. Am. Chem. Soc.* **1993**, *115*, 4844–4848.

(20) (a) Cheng, X.; Fenselau, C. *Int. J. Mass Spectrom. Ion Processes* **1992**, *122*, 109–119. (b) Suckau, D.; Shi, Y.; Beu, S. C.; Senko, M. W.; Quinn, J. P.; Wampler, F. M., III; McLafferty, F. W. *Proc. Natl. Acad. Sci. U.S.A.* **1993**, *90*, 790–793. (c) Winger, B. E.; Light-Wahl, K. J.; Smith, R. D. Proceedings of the 40th ASMS Conference on Mass Spectrometry and Allied Topics, Washington, DC, 1992; pp 481–482.

(21) (a) Loo, J. A.; Edmonds, C. G.; Udseth, H. R.; Smith, R. D. *Anal. Chem.* **1990**, *62*, 693–698. (b) Chowdhury, S. K.; Katta, V.; Chait, B. T. *J. Am. Chem. Soc.* **1990**, *112*, 9012–9013. (c) Yu, X.; Wojciechowski, M.; Fenselau, C. *Anal. Chem.* **1993**, *65*, 1355–1359.

(22) Hunt, D. F.; Sethi, S. K. *J. Am. Chem. Soc.* **1980**, *102*, 6953–6963.

